Young Talents in Polymer Science

Polymer Photocatalysts for Water Splitting: Insights from Computational Modeling

Pierre Guiglion, Cristina Butchosa, Martijn A. Zwijnenburg*

Based on insights from computational chemistry calculations, the ability of polymers to act as water splitting photocatalysts for the production of renewable hydrogen from water and sunlight is discussed. Specifically, the important role of exciton dissociation in these materials is highlighted, as well as the possible microscopic origins of the experimentally observed changes in the photocatalytic activity of a polymer with increasing chain length or changing chemical composition. The reason why water oxidation, with polymeric photocatalysts, is difficult, and which polymer properties to target when developing new polymers for water splitting photocatalysis are, finally, also discussed.

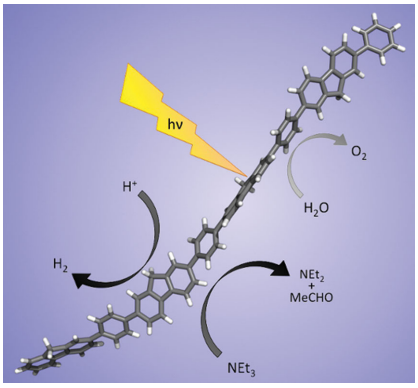

1. Introduction

Photocatalysts that split water into molecular hydrogen and oxygen when illuminated are typically inorganic crystalline semiconductors,[1–4] often combined with noble metal nanoparticles as cocatalysts. The inorganic semiconductor acts as light absorber, converting light into free electrons and holes that are thermodynamically able to drive the splitting of water or other desired reactions, while the noble metal cocatalysts lower the activation energy of the underlying elementary reaction steps and improve the kinetics in terms of conversion and selectivity.

The restriction of photocatalysts to inorganic semiconductors, however, is neither inherent nor fundamental. Already in the 1980s, it was demonstrated that oligomers and polymers of p-phenylene under illumination with UV light could catalyze the reduction of protons to hydrogen in the presence of a sacrificial electron donor.[5–7] However, the demonstration in 2009 that carbon nitride catalyzes both the reduction of protons in the presence of a sacrificial electron donor and the oxidation of water in the presence of a sacrificial electron acceptor[8] kick-started the field of polymeric photocatalysts in earnest. It spurred on the discovery of a whole range of (co-)polymers that could do the same and better.[9–30] Recently, for example, the first example of overall water splitting with a polymer photocatalyst, a carbon nitride–carbon nanodot heterostructure, was reported with 2% quantum efficiency.[25] Interestingly, in the latter example no noble metal cocatalyst was used, while also other authors found that polymers can display photocatalytic activity in the absence of (noble metal) cocatalysts[20,29,30] or in the presence of metal nanoparticles but with any potential activity of these nanoparticles inhibted

P. Guiglion, Dr. C. Butchosa, Dr. M. A. Zwijnenburg
Department of Chemistry
University College London
20 Gordon Street
London WC1H 0AJ, UK
E-mail: m.zwijnenburg@ucl.ac.uk

DOI: 10.1002/macp.201500432

by adsorbing carbon monoxide.[24] Besides their promising activity, polymeric photocatalysts also have the advantage of being based on earth abundant elements, especially for those systems that do not require a noble metal cocatalyst, and the fact that their properties can easily be tuned by copolymerization.[11,24,31]

In part because of their relative novelty, many (fundamental) properties of polymeric photocatalysts are, as yet, not very well understood. For example, there are many more polymers reported in the literature that can reduce protons than polymers that can oxidize water, and even fewer that can overall split water, raising the question whether this is the result of thermodynamic limitations or kinetic issues. There is also little known about how excitons dissociate into free electrons and holes, taking into account that such excitons are assumed to be more strongly bound in polymers than inorganic materials, and how polymer "length" influences its activity. Finally, nearly nothing is known about the underlying reaction mechanism(s). In this article, we will review what one can learn about such questions from computational modeling of polymer photocatalysts, focussing on examples from work from our group[24,29,32–34] and our experimental collaborators at the University of Liverpool: the groups of Prof. Andrew Cooper and Prof. Dave Adams.[24,29,32] We will start, however, with a brief introduction to the physical chemistry of photocatalytic water splitting.

Pierre Guiglion is a Ph.D. student in the group of Dr. Zwijnenburg at University College London studying the photocatalytic properties of polymers. He obtained his M.Sc. and Chemical Engineering degrees at the ENSCM (the National Graduate School of Chemistry of Montpellier, France) in 2011.

Cristina Butchosa has a M.Sc. and Ph.D. of the University of Girona, Spain, and worked from 2012 to 2014 as postdoctoral research assistant in the group of Dr. Zwijnenburg at University College London (UCL). Since leaving UCL, she has joined the research and development department of a Spanish manufacturer of polymeric fibers.

Martijn Zwijnenburg is a lecturer and EPSRC Career Acceleration Fellow at University College London (UCL), where he leads the Computational Photochemistry of Materials group. He obtained his Ph.D. from Delft University of Technology, The Netherlands, in 2004 and prior to joining UCL in 2010 held posts in the UK and Spain. His research interests include the prediction of the excited state properties of inorganic nanostructured, polymeric and molecular materials, the link between these excited state properties and the application of materials in applications such as photovoltaics and photocatalysis, and generating realistic structural models of materials.

2. Primer into the Physical Chemistry of Photocatalytic Water Splitting

When a polymer absorbs light of an energy larger than its optical gap (also commonly referred to as the absorption onset), electrons get excited from the highest occupied molecular orbital (HOMO, top of the valence band in a periodic crystal perspective) to the lowest unoccupied molecular orbital (LUMO, bottom of the conduction band) and excitons, excited electron–hole pairs, are formed. Such excitons can subsequently dissociate into free electrons and holes (where "free" refers to the fact that they are not bound together as part of excitons) through the supply of additional energy, the exciton binding energy. These free charge carriers can drive redox reactions, see below, but also re-form excitons in a process commonly referred to as electron–hole recombination. Both free charge carriers and excitons can also become trapped on a part of the polymer, with the structure of the polymer distorting around the free charge carrier or exciton. Excitons, finally, can decay at any stage back to the ground state via fluorescence/phosphorescence, the emission of light, or via internal conversion, a dark nonradiative route, where the excess energy is dissipated in the form of phonons (atomic vibrations).

Photocatalytic water splitting involves a combination of two *red-ox* half reactions

$$2\,H^+(aq) + 2e^- \rightarrow H_2(g) \quad (1)$$

$$O_2(g) + 4\,H^+(aq) + 4e^- \rightarrow 2H_2O(l) \quad (2)$$

where both *red-ox* half reactions are written in line with convention as reductions, and where the latter half reaction (2) runs in the opposite direction to that written above, i.e., as an oxidation rather than a reduction. In practice, many experimental studies do not investigate overall water splitting but only consider the ability of a polymer to drive one of the half reactions above, e.g., only hydrogen evolution. Such studies use a sacrificial electron donor (SED) or sacrificial electron acceptor (SEA) to provide or accept electrons and to uncouple the studied half reaction from its natural counterpart. An example of a commonly used SED is triethylamine (TEA), while Ce^{4+} salts are commonly used as SEAs. Other processes where energy rather than

electrons is transferred to molecules (water) in solution (Föster and/or Dexter energy transfer) are unlikely to be directly relevant in the case of water splitting due to the large optical gap of water (>7 eV).

For a polymer to act as a water splitting photocatalyst, it should at least be thermodynamically able to provide electrons and holes to drive both *red-ox* half reactions discussed above. This can be analyzed in terms of the potentials associated with the water splitting half reactions and those associated with free charge carriers and excitons in the polymers.[33] The half reactions for the free charge carriers and excitons are

$$P^+ + e^- \rightarrow P \quad (3)$$

$$P + e^- \rightarrow P^- \quad (4)$$

$$P^* + e^- \rightarrow P^- \quad (5)$$

$$P^+ + e^- \rightarrow P^* \quad (6)$$

where P is the neutral polymer, P* the polymer with an exciton localized on it, and P^+ and P^- the polymer with a hole in its valence band and an excess electron in the conduction band, respectively. The potential of half reaction (3) is often referred to as the polymer's ionization potential (IP) or the energy of the HOMO (or valence band maximum, VBM), while the potential of half reaction (4) is commonly referred to as the polymer's electron affinity (EA) or the energy of the LUMO (or conduction band minimum, CBM). The potentials (5) and (6) associated with the exciton can in analogy be labeled as EA* and IP*.

For water splitting to be exergonic in the presence of a polymer photocatalyst, the IP/EA* and EA/IP* potentials should straddle the water splitting half-reaction potentials (see Figure 1). This constraint enforces that for both the oxidative and reductive parts of the overall water splitting reaction, the net potential or driving force (IP/EA* – E_{Ox} and E_{Red} – EA/IP*, respectively) is positive and that the associated Gibbs free energy difference in both cases is negative.

The activity of a polymer for water splitting will not only depend on the driving force provided for both half reactions but also on the rate of photon absorption and thus exciton generation, the rate of exciton loss due to dark de-excitation and fluorescence/phosphorescence, the rate of exciton dissociation/recombination, the rate of electron and hole transfer to adsorbed molecules or cocatalysts, the wettability of the surface and the degree to which water will preferentially adsorb on the photocatalyst surface, and the kinetics of the elementary reaction steps. Under any given reaction and material preparation conditions (light spectrum & intensity, polymer particle-size, etc.) one of the terms is likely to dominate (control) the overall hydrogen and/or oxygen evolution rate. These different terms and associated parameters are also not fully independent. For example, reducing the optical gap to increase the rate of photon absorption, inevitably also means decreasing the driving force for one or both of the half reactions.

3. Insight from Computational Modeling

In the remainder we will discuss insights into polymer photocatalysts

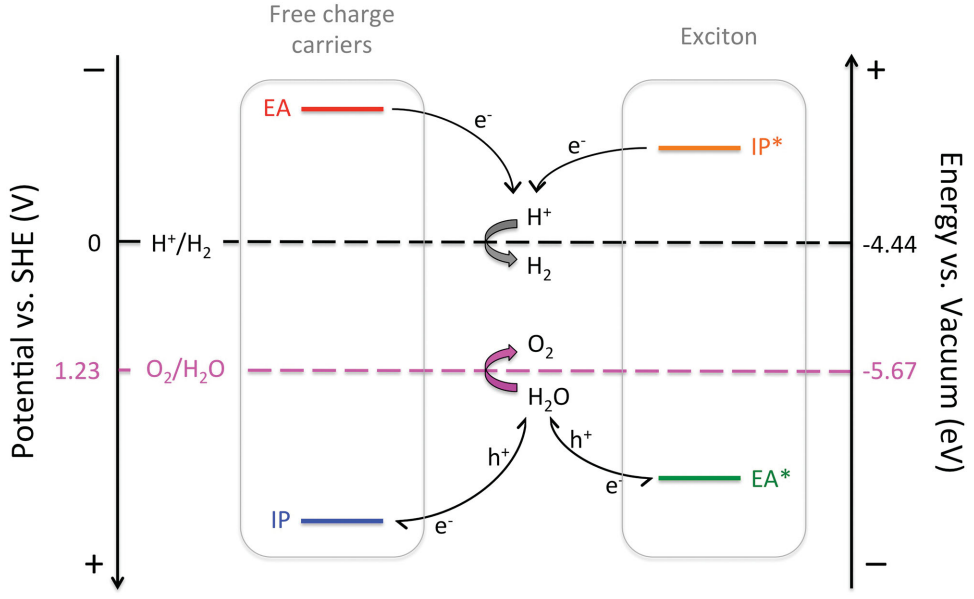

Figure 1. Scheme illustrating how the (standard) reduction potentials (IP, EA and EA* and IP*) of the ideal photocatalyst must straddle the proton reduction and water oxidation potentials (black and purple broken lines, respectively) in the case of water splitting.

for water splitting from computational modeling, focussing on examples from work from our group.[24,29,32–34] Except where explicitly stated otherwise, all calculations discussed below are based on a combination of density functional theory (DFT) and time-dependent DFT (TD-DFT), and use the B3LYP[35–38] density functional. The effect of the dielectric environment in which the polymer is embedded, critical for prediction of realistic polymer potentials, is modeled using the COSMO dielectric screening model[39] and generally a relative dielectric permittivity of 80.1, i.e., water (see Section 1 of the Supporting Information for more details).

3.1. Exciton Dissociation

Commonly, when studying photocatalysis, people only focus on processes involving free charge carriers (i.e., half reactions (3) and (4) above), implicitly assuming that excitons spontaneously dissociate and that the exciton binding energy is negligible. While this is a fair assumption for many inorganic semiconductors, for which experimentally exciton binding energies in the order of only tens of meV are measured, the same is not necessarily the case for polymers. For example, for poly(para-phenylene) (PPP), the vertical exciton binding energy (ignoring nuclear relaxation as a result of localizing a hole, electron or exciton on the polymer) is predicted to be ≈ 1200 meV in the middle of a polymer matrix and ≈ 170 meV on or near the interface with water (see Section 2 of the Supporting Information for more details). The difference between the exciton binding energies in the two scenarios arises from the fact that dielectric screening of free charges is larger in water (ε_r = 80.1) than in polymer ($\varepsilon_r \approx 2$). Such exciton binding energy values are much larger than kT at room temperature (26 meV) suggesting that excitons do not spontaneously dissociate in these polymers. Going from the vertical to the adiabatic picture, where nuclear relaxation is taken into account, does not change this picture, except near the interface with water for materials made of very short oligomers, where calculations suggest that exciton dissociation might be spontaneous.

Aside from the case of "bulk" exciton dissociation discussed above, where both the free electron and free hole after dissociation remain in the same phase, though far apart, excitons can also dissociate on the interface between two phases. This could be on the interface between different solid phases, which together form the photocatalyst, as exploited in photocatalytic heterostructures, or on the interface between the photocatalyst and the aqueous solution.[40] In both cases, one of the free charge carriers remains in the phase where the exciton was originally generated, while the other gets transferred to the other phase, and in the case of exciton dissociation on the photocatalyst–solution interface, is subsequently consumed by a solution *red-ox* reaction (see Figure 2). For example, the free hole can be transferred to the solution and take part in the oxidation of water (half reaction (2)) or a SED, while the free electron can remain on the photocatalyst, and subsequently reduce a proton (half reaction (1)). From a conceptual point of view, this exciton dissociation at the photocatalyst–solution interface is described by a combination of the photocatalyst potentials that involve the exciton (IP* and EA*, half reactions (6) and (5)) and the relevant solution red-ox potentials. If IP* is more negative than the potential of a solution red-ox reaction that accepts electrons (e.g., half reaction (1)) or EA* more positive than the potential of a solution red-ox reaction that donates electrons (e.g., half reaction (2)), exciton dissociation on the photocatalyst–solution interface will be spontaneous in terms of free energy. For many polymers/oligomers, for example melon (a linear polymer of heptazine units, see Figure 3A) and PPP (see Figure 4), this is the case for either pure water or the combination of water and a SED (methanol, triethylamine). The photocatalytic activity of such polymers can then be understood from a thermodynamic point of view as resulting from excitons dissociating at the polymer–solution interface, driving one of the solution half reactions, and generating free charge carriers in the process, to drive the other solution half reaction.

The importance of the polymer–water interface in exciton

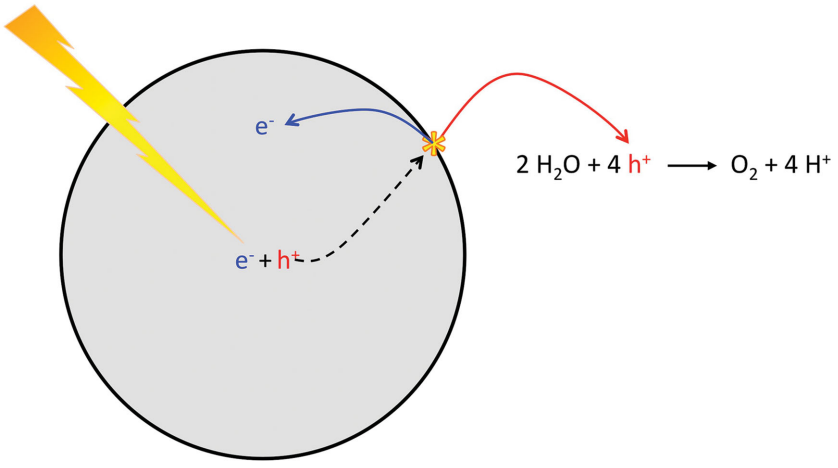

Figure 2. Illustration of exciton dissociation at the surface of a polymer particle for the case where the hole of the exciton goes into solution, where it drives water oxidation, while the electron remains on the particle.

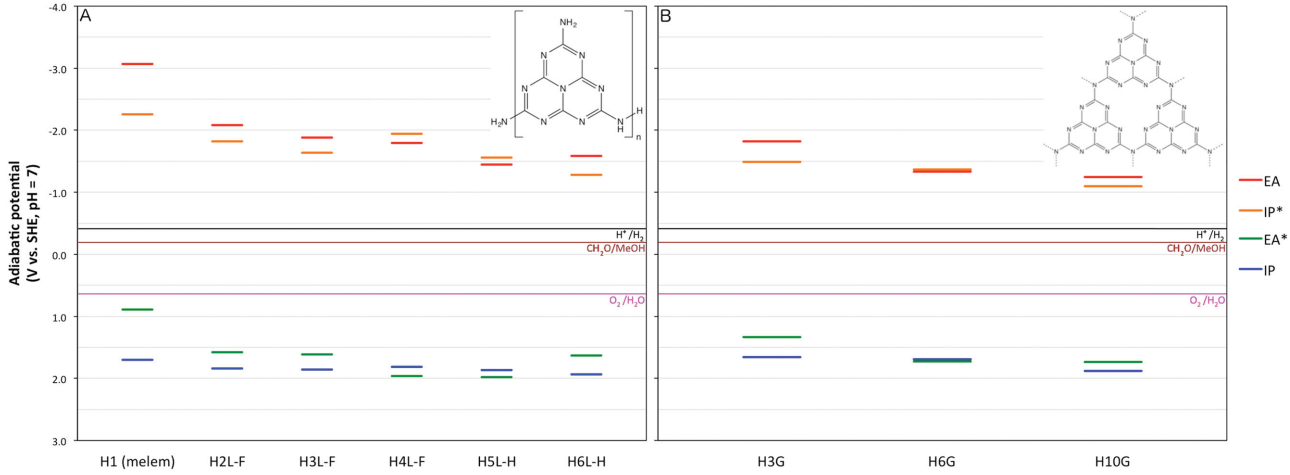

Figure 3. (TD-)B3LYP predicted IP, EA, IP*, and EA* adiabatic potentials of the lowest energy conformers of oligomers of melem (A) and graphitic carbon nitride (B) in water ($\varepsilon = 80.1$). For the melem structures, the suffixes F and H signify whether the relevant oligomers is flat or helical respectively, while all data points shown, except for melem, are taken from ref.[34].

dissociation suggests that a high surface area is a desirable property for a polymer photocatalyst to have and should result in better quantum efficiencies than photocatalyst made of the same polymer but with reduced surface area. As such, photocatalysts based on conjugated microporous polymers[24] and covalent organic frameworks,[23,41] with large internal surface areas because of their porosity, might be an attractive proposition.

3.2. Water Oxidation and Overall Water Splitting

As already touched upon in the introduction, many polymers can experimentally reduce protons and some can (also) oxidize water, but very few can perform overall photocatalytic water splitting. For example, pure carbon nitride, be it graphitic carbon nitride or melon, is know experimentally to reduce protons in the presence of a SED and oxidize water when a SEA is present, but not split pure water.[8] Oligomers of PPP and the PPP polymer[5–7,29] in contrast, are only known to reduce protons. The question is whether the apparent inability to drive overall water splitting and/or one of the two solution half reactions in the presence of a SED/SEA is inherent to the material in question, or dependent on the reaction conditions, the size and morphology of the material and/or the presence of cocatalysts.

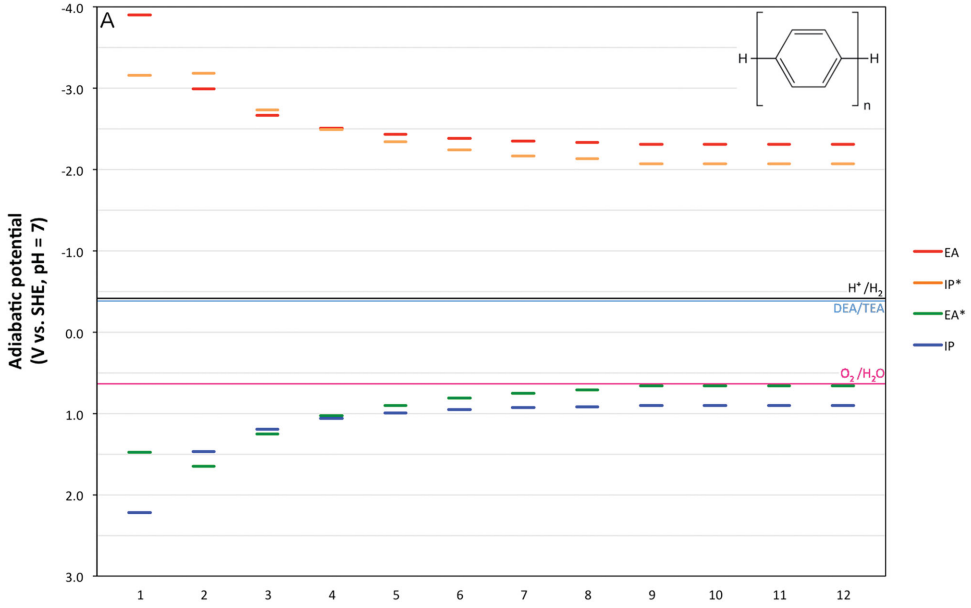

Figure 4. (TD-)B3LYP predicted IP, EA, IP*, and EA* adiabatic potentials of the lowest energy conformers of oligomers of PPP, of lengths n = 1 to n = 12, in water ($\varepsilon = 80.1$). All data points shown, except for benzene, are taken from ref.[33]

Focussing on PPP and carbon nitride as an example, a comparison of Figure 3A,B (which shows the potentials for graphitic carbon nitride), and Figure 4A, suggests that this difference might arise from the fact that the oxidative potentials (IP/EA*) of PPP oligomers, and of the PPP polymer by extrapolation, are much more negative than that of the carbon nitride materials. Specifically, our calculations predict that water oxidation is exergonic for the carbon nitride materials (in line with other more approximate band-structure-based calculations for graphitic carbon nitride[8,42]) but endergonic or borderline exergonic for PPP. Similarly, the driving force for methanol oxidation to formaldehyde is much larger in the case of the carbon nitride structures than for PPP, perhaps explaining why methanol can be used experimentally as a SED for carbon nitride,[20,21,26] but only results in negligible hydrogen evolution in the case of PPP.[5,29] Finally, the driving force for triethylamine oxidation to diethylamine (DEA) and acetaldehyde is substantial for both sets of materials, explaining why it, in contrast to methanol, can be used as a SED for proton reduction with both carbon nitride materials[43] and PPP.[5–7,29]

The observations above suggest that the lack of experimental overall water splitting of pure carbon nitride is a kinetic issue, arising from the competition between four-hole water oxidation and electron–hole recombination. This is probably why combining carbon nitride in a heterostructure with an otherwise inert material (polypyrrole,[16] carbon nanodots[25] results in the combined material driving overall photocatalytic water splitting. The heterostructure separates electrons and holes, increases their lifetime and results in the solution half reactions being competitive with electron–hole recombination, even if the underlying details are still poorly understood.[34] Oxidation of SEDs is not only easier because of the more negative potentials associated with them but also because they typically require two rather than four holes. The issue with PPP, in contrast, appears inherent to the material and thermodynamic in origin, and as a result, it can only find use in overall water splitting as part of a two-photon Z-scheme.[2,4]

3.3. Oligomers Versus Polymers

It is well known that the optical properties of oligomers such as the optical gap and fluorescence energy evolve with chain length until converging to their polymer values in the long chain limit. It is perhaps then also not surprising that the same holds true for the polymer potentials. Figures 3A and 4A show how the polymer potentials change with chain length for melon and PPP. For all systems, the gap between the reductive and oxidative potentials decreases with increasing chain length. This reduction is linked to the similar decrease in optical gap and fundamental gap (the optical gap plus the exciton binding energy, also referred to as band gap) with oligomer length, since in the vertical approximation the difference between IP and EA is by definition equal to the fundamental gap, and that between IP* and IP (and EA and EA*) to the optical gap (see Figure 5). For the same reason, both the driving force for reduction (EA/IP*) and oxidation (IP/EA*) generally decrease with oligomer length, i.e., the potentials shift to more positive and more negative values, respectively. The trends appear slightly more systematic for oligomers where the structures of the lowest energy conformers are similar, e.g., PPP, than where they change with oligomer length, e.g., melon, but they are present for every linear polymer we studied. This overall analysis is supported by limited experimental cyclic voltammetry data available in the literature for PPP[44] and melem[45] oligomers derivatized with bulky alkyl groups. It is thus apparent that generally, the thermodynamic driving force for both of the solution red-ox reaction decreases with chain length.

The reduction in thermodynamic driving force is, however, only one

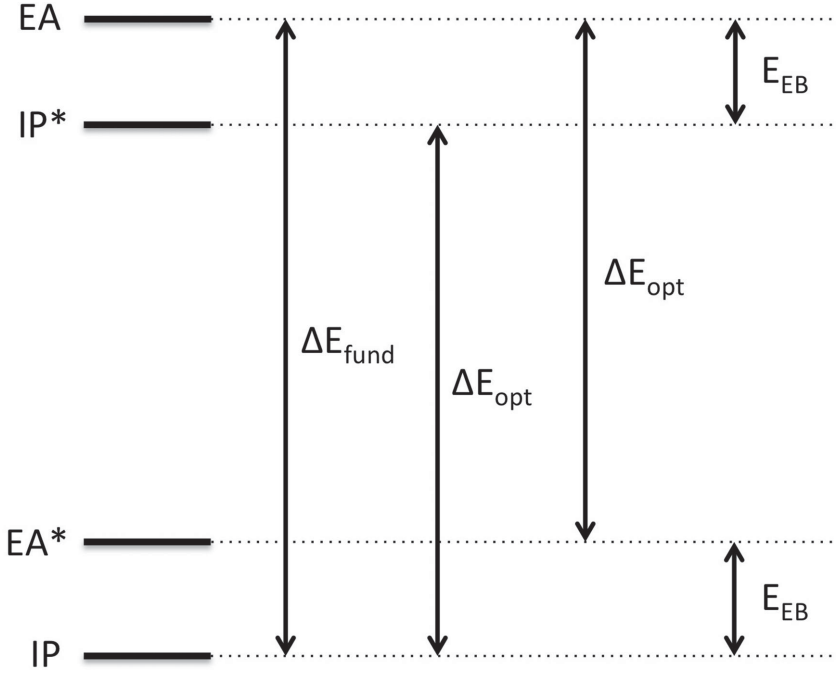

Figure 5. Scheme illustrating the connection between the vertical potentials and the fundamental (or band) gap ΔE_{fund}, the optical gap ΔE_{opt} and the exciton binding energy E_{EB}.

of the effects of increasing the chain length. For most polymers, including melon[34] and PPP,[44,46–49] the optical gap decreases with increasing chain length and thus in principle, a larger fraction of the spectrum of the light illuminating the polymer can be absorbed, and more photons converted into excitons (increased rates of photon absorption and exciton generation), subsequently generating more free charge carriers and ultimately more molecular hydrogen and oxygen. There might also be an effect of chain length on the lifetime of excitons (reduction in exciton loss rate) and free charge carriers (reduction in exciton recombination rate), although that is more difficult to explore computationally.

It is then interesting to compare our calculations on melon and PPP with experimental data for hydrogen evolution in these systems. For melon, Lau et al.[26] found that when separating the as-synthesized material in weight fractions by ultracentrifugation, the fractions containing predominantly short melon oligomers evolved more hydrogen from an aqueous methanol solution under visible illumination than the as-synthesized sample also containing longer oligomers on a weight for weight basis. More specifically, they found that the hydrogen evolution rate was smallest for the as as-synthesized sample, higher for the fraction containing predominantly trimers, and highest for the fraction containing predominantly dimers. However, melem, consisting of a single heptazine unit, evolves less hydrogen than all other samples under the same conditions. Based on the calculated potentials in Figure 3A, the increase in hydrogen evolution with decreasing chain length can be explained by the increase in driving force for proton reduction. Alternatively, one could suppose that the amino ($–NH_2$) groups act as an active site for hydrogen evolution and that the increase in hydrogen evolution might somehow be (partially) linked to an increase in the amino-group-to-heptazine ratio with decreasing oligomer length. Melon is predicted to have an even bigger driving force (as well as a higher amino-group-to-heptazine ratio) than the melon oligomers but, while the dimer and trimer still absorb light in the visible spectrum (≈ 3.1 eV experimentally and ≈ 3.5 eV predicted by TD-B3LYP), the absorption onset of melem (≈ 3.7 eV experimentally and 4.1 eV predicted by TD-B3LYP) is shifted into the UV, meaning that only few visible photons will be absorbed and the rate of hydrogen evolution significantly reduced. The dependence of the hydrogen evolution rate of melon oligomers on the chain length thus appears to correspond to the scenario discussed above. The nature of the material property that controls the photocatalytic activity changes with oligomer size, from the magnitude of the thermodynamic driving force, to the rate of photon absorption, resulting in a maximum in the hydrogen evolution rate.

In the case of PPP, Matsuoka et al.[7] found that the polymer evolves more hydrogen than any of the oligomers, from an aqueous solution containing both methanol and triethylamine illuminated with UV light (both in the presence of $RuCl_3$ or Ru nanoparticles as cocatalyst). Moreover, they also observed a nonsystematic trend with chain length for the PPP oligomers, where the trimer evolved more hydrogen than either the dimer or the longer oligomers. In more recent work by our collaborators at the University of Liverpool,[29] where a similar aqueous solution was illuminated with UV light but without the addition of a cocatalyst, it was also found that the PPP polymer evolves more hydrogen than the oligomers, but, in contrast to Matsuoka et al., a systematic trend between the amount of hydrogen evolved and chain length was also observed for the oligomers. These PPP results suggest that, at least under these reaction conditions, hydrogen evolution is not controlled by the thermodynamic driving force, which as can be seen in Figure 4A is predicted to decrease with increasing chain length, but rather by the decrease in optical gap with increasing chain length. The fact that the PPP polymer evolves much more hydrogen than the oligomers in both cases, finally, strongly suggests that hydrogen evolution in the polymer is controlled by yet another factor, possibly an increased lifetime of free charge carriers.

Beyond linear polymers, similar relationships between the photocatalytic properties of polymers and their spatial extent in two or three dimensions are also expected to exist for network-like polymers, such as conjugated microporous polymers, covalent organic frameworks, and layered polymers. Indeed, Figure 3B shows that for graphitic carbon nitride the potentials shift with increasing size of the nanoflake.

3.4. Heteroatom Substitution

Besides changing the chain length, altering the chemical composition of a polymer provides an alternative pathway to tuning the photocatalytic properties of polymers. From the potentials in Figures 3 and 4, for example, it is clear that carbon nitride in the long polymer limit has a substantially deeper IP/EA* than the purely hydrocarbon PPP and PFP materials. As previously mentioned, this can be linked to the experimental observation that carbon nitride can oxidize either water, as part of a heterostructure, or methanol, when on its own, while PPP can only oxidize the SED triethylamine, which is much easier to do from a thermodynamic perspective.

Calculation of the potentials of long oligomers of poly(2,7-pyrene) (PPyre) and poly(p-phenylene vinylene) (PPV), shown in Figure 6, suggests

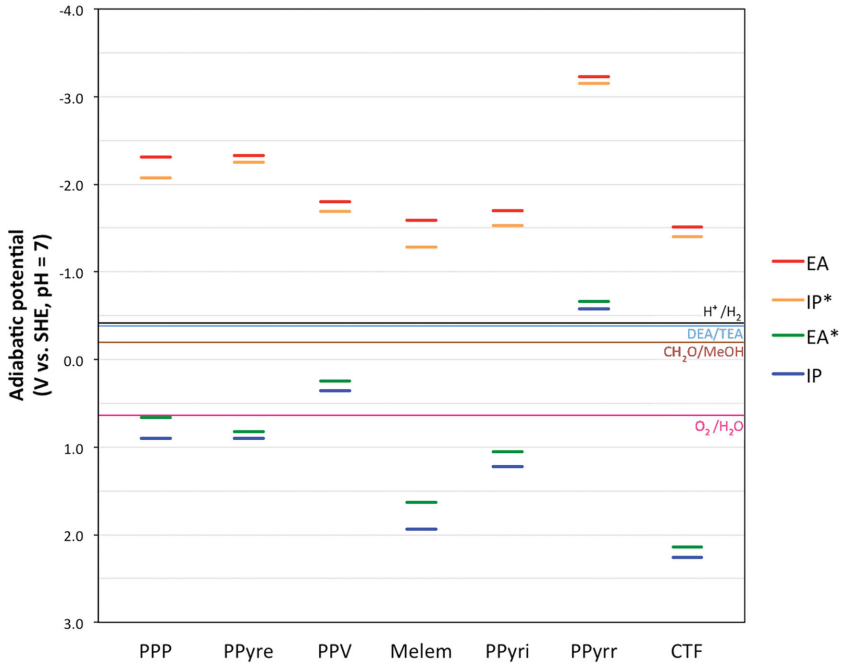

Figure 6. (TD-)B3LYP predicted IP, EA, IP*, and EA* adiabatic potentials of a range of linear polymers in the long polymer limit (for abbreviation, see text, all calculations on oligomers of 12 phenylene equivalent units), as well as a melon hexamer (H6L-H) and a 6-ring cluster model of the CTF-1 structure, in water ($\varepsilon = 80.1$).

that while purely hydrocarbon polymers will all have different potentials, none of their IP/EA* potentials will ever lie deep enough to oxidize water. In contrast, introduction of nitrogen heteroatoms, in analogy to carbon nitride, appears a promising strategy for shifting the IP/EA* potentials to more positive (deeper) values while maintaining sufficiently negative (shallow) EA/IP* potentials to drive hydrogen evolution. The IP/EA* potentials of poly(pyridine-2,5-diyl) (PPyri),[33] a nitrogen-substituted version of PPP with one nitrogen heteroatom per phenyl ring that experimentally has been shown to evolve hydrogen from an aqueous solution of triethylamine in the presence of Ru or Pd as cocatalyst,[9,50] lie in Figure 6 between those of PPP and melon (in line with photoelectron spectroscopy data for PPP and PPyri[51]). While the IP/EA* potentials of phenyl-triazine materials, be it phenyl-triazine oligomers[27] or covalent triazine-based frameworks (CTF-1),[28,31,52] both of which have been shown to evolve hydrogen from aqueous solutions of SEAs,[27,28] are likely to be shifted to even more positive values than those of melon, based on the values calculated (see Figure 6, as well as approximate band-structure-based calculations by Jiang et al.[53]) for a 6-ring R6[32] fragment of CTF-1 (see Figure S2 in the Supporting Information for the structure of this fragment). The latter is in line with the fact that CTF-1, just as carbon nitride, is reported to not only evolve hydrogen but also oxygen from a SED-containing solution.[28]

Nitrogen-containing polymers are, however, no panacea. The IP/EA* potentials of polypyrrole (PPyrr) are even considerably shallower than the purely hydrocarbon polymers, suggesting it cannot even oxidize typical SEAs. The widely different effect of nitrogen probably depends on whether its incorporation give rise to an electron-rich π system, e.g., in the case of pyrrole, or an electron-poor π system, e.g., for pyridine and triazine.

The presence of heteroatoms also has other effects on the polymer properties relevant to photocatalysis. Some of these are easily probed by computational chemistry; e.g., the reduction of the optical gap (the optical gap of PPP-12 and PPyri-12 in vacuum are predicted to be 3.46 and 2.93 eV, respectively) and likely increase in photon absorption rate. Others, like changes in the rates of exciton dissociation and the kinetics of elementary reaction steps, as well the wettability of the polymer surface by water and thus the local water concentration near the surface in multi-component multi-phase solutions (e.g., SED solutions or water + gas bubbles), are harder to study computationally.

4. Outlook

Above we discussed how the photocatalytic properties of polymers can be tuned by varying the spatial extent of polymers and/or changing its chemistry, where the incorporation of nitrogen appears to be an especially promising strategy. The only two polymer systems, as far as we are aware of, that can oxidize water in the presence of a SEA, carbon nitride and CTF-1, both contain aromatic rings with more than one nitrogen heteroatom per ring. We would also not be surprised if CTF-1 combined with a suitable other material in a heterostructure, would act as an overall water splitting photocatalyst, just as carbon nitride–carbon nanodot heterostructures. It is evident that this ability of nitrogen-containing polymers to oxidize water is directly linked to the deep IP/EA* potentials of these materials and the fact that water oxidation by these materials is thus exergonic.

The effect of changing a polymer's spatial extent appears more subtle and less clear cut. While tuning the chemical composition can turn a polymer that does not oxidize water into one that does, changing the spatial extent changes (only) the

hydrogen evolution rate. Different materials display different trends with system size, e.g., for the linear polymers PPP and PFP, an increase of hydrogen evolution with chain length and a decrease in the case of melem. We believe these different trends are due to the fact that catalytic activity of a polymer is a sum of many contributions (e.g., exciton generation rate, rate of exciton dissociation, rate of electron–hole recombination, etc.) and that the nature of dominant contribution, which is the rate controlling step, will depend on the chemical composition of the polymer and the polymer's spatial extent, as well as the reaction conditions.

Taking into account the rather binary effect of changing the chemical composition and the fact that most known polymers have too shallow IP/EA* potentials for water oxidation, including most polymer originally developed for organic photovoltaics, we believe that there is a strong impetus for a combined computational and experimental effort to find new (co-)polymers that can drive water oxidation. Such work, if successful, would not only significantly increase the numbers of polymers that can potentially catalyze the overall splitting of water, either alone or as part of a heterostructure, but also play to the strengths of the computational and experimental methods available to screen for such materials. The other area of polymer photocatalysis that we believe deserves special attention and could benefit from a combined computational and experimental effort is the physics and chemistry that underlie the electron–hole separation in heterostructures and the origin of their activity for the overall splitting of water.

Supporting Information

Supporting Information is available from the Wiley Online Library or from the author.

Acknowledgements: The authors would like to thank their collaborators at the University of Liverpool: Prof. D. J. Adams, Dr. B. Bonillo, Prof. A. I. Cooper, and Dr. R. S. Sprick for valuable insights into the challenges of preparing and characterizing polymeric photocatalysts, as well as the willingness to test the authors' predictions. The authors also kindly acknowledge Dr. M. Bojdys, Dr. H. Bronstein, Dr. L. Chen, Dr. A. Cowan, Dr. F. Cora, Dr. J. Gierschner, Dr. T. Hasell, Prof. B. Lotsch, Prof. P. F. M. McMillan, Prof. J. Nelson, Dr. B. J. Slater, and Dr. M. Wykes for stimulating discussions. M.A.Z. thanks the UK Engineering and Physical Sciences Research Council (EPSRC) for a Career Acceleration Fellowship (Grant No. EP/I004424/1) and for their support for the joint efforts of the experimental collaborators in Liverpool and us (Grant No. EP/N004884/1).

Received: October 12, 2015; Revised: November 23, 2015; Published online: December 30, 2015; DOI: 10.1002/macp.201500432

Keywords: conjugated polymer; carbon nitride; density functional theory; photocatalysis; water splitting

[1] A. Kudo, Y. Miseki, *Chem. Soc. Rev.* **2009**, *38*, 253.
[2] K. Maeda, K. Domen, *J. Phys. Chem. Lett.* **2010**, *1*, 2655.
[3] F. E. Osterloh, *Chem. Soc. Rev.* **2013**, *42*, 2294.
[4] T. Hisatomi, J. Kubota, K. Domen, *Chem. Soc. Rev.* **2014**, *43*, 7520.
[5] S. Yanagida, A. Kabumoto, K. Mizumoto, C. Pac, K. Yoshino, *J. Chem. Soc., Chem. Commun.* **1985**, 474.
[6] T. Shibata, A. Kabumoto, T. Shiragami, O. Ishitani, C. Pac, S. Yanagida, *J. Phys. Chem.* **1990**, *94*, 2068.
[7] S. Matsuoka, H. Fujii, T. Yamada, C. Pac, A. Ishida, S. Takamuku, M. Kusaba, N. Nakashima, S. Yanagida, *J. Phys. Chem.* **1991**, *95*, 5802.
[8] X. C. Wang, K. Maeda, A. Thomas, K. Takanabe, G. Xin, J. M. Carlsson, K. Domen, M. Antonietti, *Nat. Mater.* **2009**, *8*, 76.
[9] T. Maruyama, T. Yamamoto, *J. Phys. Chem. B* **1997**, *101*, 3806.
[10] M. G. Schwab, M. Hamburger, X. Feng, J. Shu, H. W. Spiess, X. Wang, M. Antonietti, K. Müllen, *Chem. Commun.* **2010**, *46*, 8932.
[11] J. Zhang, X. Chen, K. Takanabe, K. Maeda, K. Domen, J. D. Epping, X. Fu, M. Antonietti, X. Wang, *Angew. Chem. Int. Ed.* **2010**, *49*, 441.
[12] Z. Zhang, J. Long, L. Yang, W. Chen, W. Dai, X. Fu, X. Wang, *Chem. Sci.* **2011**, *2*, 1826.
[13] Y. Cui, Z. Ding, X. Fu, X. Wang, *Angew. Chem. Int. Ed.* **2012**, *51*, 11814.
[14] S. Chu, Y. Wang, Y. Guo, P. Zhou, H. Yu, L. Luo, F. Kong, Z. Zou, *J. Mater. Chem.* **2012**, *22*, 15519.
[15] Z. Hong, B. Shen, Y. Chen, B. Lin, B. Gao, *J. Mater. Chem. A* **2013**, *1*, 11754.
[16] Y. Sui, J. Liu, Y. Zhang, X. Tian, W. Chen, *Nanoscale* **2013**, *5*, 9150.
[17] K. Schwinghammer, B. Tuffy, M. B. Mesch, E. Wirnhier, C. Martineau, F. Taulelle, W. Schnick, J. Senker, B. V. Lotsch, *Angew. Chem. Int. Ed.* **2013**, *52*, 2435.
[18] K. Kailasam, J. Schmidt, H. Bildirir, G. Zhang, S. Blechert, X. Wang, A. Thomas, *Macromol. Rapid Commun.* **2013**, *34*, 1008.
[19] L. Ge, C. Han, X. Xiao, L. Guo, Y. Li, *Mater. Res. Bull.* **2013**, *48*, 3919.
[20] A. B. Jorge, D. J. Martin, M. T. S. Dhanoa, A. S. Rahman, N. Makwana, J. W. Tang, A. Sella, F. Cora, S. Firth, J. A. Darr, P. F. McMillan, *J. Phys. Chem. C* **2013**, *117*, 7178.
[21] S. Chu, Y. Wang, Y. Guo, J. Feng, C. Wang, W. Luo, X. Fan, Z. Zou, *ACS Catal.* **2013**, *3*, 912.
[22] D. J. Martin, K. Qiu, S. A. Shevlin, A. D. Handoko, X. Chen, Z. Guo, J. Tang, *Angew. Chem. Int. Ed.* **2014**, *53*, 9240.
[23] L. Stegbauer, K. Schwinghammer, B. V. Lotsch, *Chem. Sci.* **2014**, *5*, 2789.
[24] R. S. Sprick, J.-X. Jiang, B. Bonillo, S. Ren, T. Ratvijitvech, P. Guiglion, M. A. Zwijnenburg, D. J. Adams, A. I. Cooper, *J. Am. Chem. Soc.* **2015**, *137*, 3265.
[25] J. Liu, Y. Liu, N. Liu, Y. Han, X. Zhang, H. Huang, Y. Lifshitz, S.-T. Lee, J. Zhong, Z. Kang, *Science* **2015**, *347*, 970.
[26] V. W.-H. Lau, M. B. Mesch, V. Duppel, V. Blum, J. Senker, B. V. Lotsch, *J. Am. Chem. Soc.* **2015**, *137*, 1064.
[27] K. Schwinghammer, S. Hug, M. B. Mesch, J. Senker, B. V. Lotsch, *Energy Environ. Sci.* **2015**, *8*, 3345.
[28] J. Bi, W. Fang, L. Li, J. Wang, S. Liang, Y. He, M. Liu, L. Wu, *Macromol. Rapid Commun.* **2015**, *36*, 1799.
[29] R. S. Sprick, B. Bonillo, R. Clowes, P. Guiglion, N. J. Brownbill, B. J. Slater, F. Blanc, M. A. Zwijnenburg, D. J. Adams, A. I. Cooper, *Angew. Chem. Int. Ed.* **2016**, DOI: 10.1002/anie.201510542.
[30] G. Zhang, C. Ni, L. Liu, G. Zhao, F. Fina, J. T. S. Irvine, *J. Mater. Chem. A* **2015**, *3*, 15413.

[31] J.-X. Jiang, A. Trewin, D. J. Adams, A. I. Cooper, *Chem. Sci.* **2011**, *2*, 1777.
[32] C. Butchosa, T. O. McDonald, A. I. Cooper, D. J. Adams, M. A. Zwijnenburg, *J. Phys. Chem. C* **2014**, *118*, 4314.
[33] P. Guiglion, C. Butchosa, M. Zwijnenburg, *J. Mater. Chemi. A* **2014**, *2*, 11996.
[34] C. Butchosa, P. Guiglion, M. A. Zwijnenburg, *J. Phys. Chem. C* **2014**, *118*, 24833.
[35] S. H. Vosko, L. Wilk, M. Nusair, *Can. J. Phys.* **1980**, *58*, 1200.
[36] C. Lee, W. Yang, R. G. Parr, *Phys. Rev. B* **1988**, *37*, 785.
[37] A. D. Becke, *J. Chem. Phys.* **1993**, *98*, 5648.
[38] P. J. Stephens, F. J. Devlin, C. F. Chabalowski, M. J. Frisch, *J. Phys. Chem.* **1994**, *98*, 11623.
[39] A. Klamt, G. Schüürmann, *J. Chem. Soc., Perkin Trans.2*, **1993**, 799.
[40] E. Berardo, M. A. Zwijnenburg, *J. Phys. Chem. C* **2015**, *119*, 13384.
[41] V. S. Vyas, F. Haase, L. Stegbauer, G. Savasci, F. Podjaski, C. Ochsenfeld, B. V. Lotsch, *Nat. Commun.* **2015**, *6*, 8508.
[42] K. Srinivasu, B. Modak, S. K. Ghosh, *J. Phys. Chem. C* **2014**, *118*, 26479.
[43] Z. Zeng, K. Li, L. Yan, Y. Dai, H. Guo, M. Huo, Y. Guo, *RSC Adv.* **2014**, *4*, 59513.
[44] M. Banerjee, R. Shukla, R. Rathore, *J. Am. Chem. Soc.* **2009**, *131*, 1780.
[45] A. Zambon, J. M. Mouesca, C. Gheorghiu, P. A. Bayle, J. Pecaut, M. Claeys-Bruno, S. Gambarelli, L. Dubois, *Chem. Sci.* **2015**, DOI: 10.1039/C5SC02992A.
[46] C. Seoul, W.-J. Song, G.-W. Kang, C. Lee, *Synth. Met.* **2002**, *130*, 9.
[47] V. Lukeš, A. J. A. Aquino, H. Lischka, H.-F. Kauffmann, *J. Phys. Chem. B* **2007**, *111*, 7954.
[48] K. Park, T.-W. Lee, M.-J. Yoon, J.-I. Choe, *Bull. Korean Chem. Soc.* **2014**, *35*, 531.
[49] P. Guiglion, M. A. Zwijnenburg, *Phys. Chem. Chem. Phys.* **2015**, *17*, 17854.
[50] S. Matsuoka, T. Kohzuki, Y. Kuwana, A. Nakamura, S. Yanagida, *J. Chem. Soc., Perkin Trans.2*, **1992**, 679.
[51] T. Miyamae, D. Yoshimura, H. Ishii, Y. Ouchi, K. Seki, T. Miyazaki, T. Koike, T. Yamamoto, *J. Chem. Phys.* **1995**, *103*, 2738.
[52] P. Kuhn, M. Antonietti, A. Thomas, *Angew. Chem. Int. Ed.* **2008**, *47*, 3450.
[53] X. Jiang, P. Wang, J. Zhao, *J. Mater. Chem. A* **2015**, *3*, 7750.